

## LINEAR OR NONLINEAR FRACTURE MECHANICS OF CONCRETE?

G. A. Plizzari

Dept. of Civil Engineering, University of Brescia, Brescia, Italy

V. E. Saouma

Dept. of Civil Environmental & Architectural Engineering, University of Colorado, Boulder, CO, USA

### Abstract

This paper addresses a fundamental problem that is at the root of the applicability of fracture mechanics to concrete. On the basis of theoretical considerations, it quantifies the error introduced by a simple LEFM analysis vis a vis of a more comprehensive (albeit complex) NLFM one. The error is expressed in terms of peak load, which is the primary metric of practical interest to engineers.

### 1 Introduction

In the early days, fracture mechanics of concrete borrowed extensively from the linear elastic fracture mechanics (LEFM) of metals. However, it was soon discovered that due to the presence of the fracture process zone (FPZ) at the tip of a crack, LEFM may not necessarily be applicable. In particular, when the size of the FPZ is appreciably less than the characteristic dimension  $D$  of the structure, crack extension can be quantified using LEFM procedures, otherwise, a nonlinear fracture mechanics (NLFM) analysis should

be performed. However, computational tools for NLFM analyses are not yet widely available, and yet engineers might be confronted with the task of analyzing a cracked concrete structure.

Subsequently, various guidelines have been proposed to determine modified LEFM parameters or the conditions under which LEFM is applicable (Carpinteri, 1982; Hillerborg, 1985; Shah and Jenq, 1985; Bažant et al., 1986).

Whereas fracture mechanics of concrete has been under continuous and active investigation for over fifteen years, there is little doubt that it is of most relevance in those structures where there is little or no reinforcement. In fact, properly engineered reinforced concrete structures are designed in such a way that reinforcement will transfer most, if not all, the load originally carried by concrete under tension. Prime examples of unreinforced concrete structures are dams, locks, and bulk-heads, which are large concrete structures. It is the authors' opinion that those structures are indeed prime candidates for the application of fracture mechanics, be it linear or nonlinear.

In large structures, because of the smaller size of the FPZ, limited errors should occur under the assumption of LEFM and, in engineering analyses, limited errors are acceptable as long as they are known. Therefore, it is useful to develop a procedure that would provide engineers with an approximate value of the error incurred by a LEFM analysis, and compare it with the accepted errors related to other basic properties such as compressive strength and applied load.

In this paper, through theoretical considerations based on size effect laws for LEFM and NLFM, a simple geometry independent equation is proposed to assess the error encountered in performing a LEFM analysis of a large concrete structure. The theoretical curves are first derived, and then contrasted with results of several finite element analyses.

## 2 Theoretical considerations

According to LEFM, the stress singularity at the crack tip of a solid with a crack of length  $a_0$  is characterized by the stress intensity factor

$$K_I = \sigma_N \sqrt{D} f(\alpha_0) \quad (1)$$

where:  $D$  is the characteristic dimension of the structure,  $f(\alpha_0)$

is a dimensionless geometry shape function,  $\alpha_0 = a_0/D$  is the dimensionless crack length and  $\sigma_N$  is the nominal stress that, in two dimensional structures subjected to a point load  $P$ , can be generically expressed as  $\sigma_N = P/bD$  where  $b$  is the specimen thickness. The maximum load is attained when  $K_I$  reaches the fracture toughness of the material  $K_{Ic} = \sqrt{E'G_F}$  and it can be expressed in terms of nominal stress

$$\sigma_{N,D}^{\text{LEFM}} = \left( \frac{E'G_F}{Dg(\alpha_0)} \right)^{\frac{1}{2}} \quad (2)$$

where:  $G_F$  is the energy required for crack growth,  $E' = E$  for plane stress and  $E' = E/(1 - \nu^2)$  for plane strain,  $E$  being Young's modulus,  $\nu$  being Poisson's ratio,  $g(\alpha_0) = f^2(\alpha_0)$  and  $\sigma_{N,D}^{\text{LEFM}} = P_{\text{max}}^{\text{LEFM}}/bD$ . In subsequent derivations, we attach the subscript  $D$  to indicate that the nominal stress depends on the characteristic dimension; also, we refer to plane stress problems (the solution for plane strain problems can be obtained by following a similar procedure).

Eq. 2 can be rewritten in a dimensionless form as

$$\frac{\sigma_{N,D}^{\text{LEFM}}}{f_t'} = \left( \frac{1}{\frac{D}{l_{ch}}g(\alpha_0)} \right)^{\frac{1}{2}} = \left( \frac{1}{\frac{D^*}{l_{ch}}} \right)^{\frac{1}{2}} \quad (3)$$

where  $D^* = Dg(\alpha_0)$  is the LEFM geometry independent characteristic dimension of the specimen and  $l_{ch} = \frac{EG_F}{f_t'^2}$  is the characteristic length of the material (Hillerborg et al., 1976). Hence, Eq. 3 represents the scale law for structures within the framework of LEFM and it shows that the normalized nominal maximum stress is inversely proportional to the square root of the characteristic dimension of the structure.

Let us consider now an elastic-softening structure, with positive geometry (i.e. the shape function  $f(\alpha)$  increases with crack extension), containing a crack with an initial length  $a_0$  and characteristic dimension  $D$ ; according to Planas and Elices (1988) and Bažant's size effect law (Bažant, 1984; Bažant and Kazemi, 1990), the geometry independent nominal maximum stress  $\bar{\sigma}_{N,D}^{\text{NLFM}}$  is

$$\bar{\sigma}_{N,D}^{\text{NLFM}} = \sqrt{g'(\alpha_0)}\sigma_{N,D}^{\text{NLFM}} = \left( \frac{E'G_F}{c_f + \frac{g(\alpha_0)}{g'(\alpha_0)}D} \right)^{\frac{1}{2}} = \left( \frac{E'G_F}{c_f + D^{**}} \right)^{\frac{1}{2}} \quad (4)$$

where  $\sigma_{N,D}^{NLFM} = P_{\max}^{NLFM} / bD$ ,  $g'(\alpha_0)$  is the first derivative of  $g(\alpha)$  evaluated at  $\alpha = \alpha_0$ ,  $c_f$  is the elastically equivalent crack extension at peak load in an infinitely large structure (Bažant and Kazemi, 1990; Planas and Elices, 1991), and  $D^{**} = Dg(\alpha_0)/g'(\alpha_0)$  represents the geometry independent characteristic dimension of the structure. Eq. 4 is strictly applicable when  $c_f$  is small compared with  $D$  (as in large structures) and gives an approximation of the maximum nominal stress for larger  $c_f/D$  ratios (Smith, 1995).

Since the applicability of the NLFM to concrete structures depends essentially on the size of the specimen relative to the FPZ size, which in turn depends on the material characteristic length  $l_{ch}$ , it is worth to normalize the structure size to  $l_{ch}$ . This can be obtained from Eq. 4 by normalizing the nominal stress to the tensile strength  $f'_t$

$$\frac{\bar{\sigma}_{N,D}^{NLFM}}{f'_t} = \left( \frac{1}{\frac{c_f}{l_{ch}} + \frac{D^{**}}{l_{ch}}} \right)^{\frac{1}{2}} \quad (5)$$

Since  $c_f$  is a material property (Bažant and Kazemi, 1990), and depends on the shape of the softening curve (Planas and Elices, 1991), it could be expressed as

$$c_f = \kappa_f l_{ch} \quad (6)$$

where  $l_{ch}$  takes into account the mechanical properties of the material and  $\kappa_f$  is a dimensionless parameter which takes into account the shape of the softening law.

Hence, Eqs. 5 can be rewritten as

$$\frac{\bar{\sigma}_{N,D}^{NLFM}}{f'_t} = \left( \frac{1}{\kappa_f + \frac{D^{**}}{l_{ch}}} \right)^{\frac{1}{2}} \quad (7)$$

Revisiting Eq. 3, it can also be expressed in terms of  $D^{**}$ , and of nominal stress  $\bar{\sigma}_{N,D}$

$$\frac{\bar{\sigma}_{N,D}^{LEFM}}{f'_t} = \sqrt{g'(\alpha_0)} \frac{\sigma_{N,D}^{LEFM}}{f'_t} = \left( \frac{1}{\frac{D^{**}}{l_{ch}}} \right)^{\frac{1}{2}} \quad (8)$$

so that the ratio between the maximum loads obtained from a LEFM and NLFM analyses (Eqs. 8 and 7), which varies with the structure dimension, can be expressed by

$$\frac{\bar{\sigma}_{N,D}^{LEFM}}{\bar{\sigma}_{N,D}^{NLFM}} = \frac{\sigma_{N,D}^{LEFM}}{\sigma_{N,D}^{NLFM}} = \frac{P_{\max}^{LEFM}}{P_{\max}^{NLFM}} = \left( 1 + \frac{\kappa_f}{\frac{D^{**}}{l_{ch}}} \right)^{\frac{1}{2}} = \left( 1 + \frac{c_f}{D^{**}} \right)^{\frac{1}{2}} \quad (9)$$

Eq. 9, valid for all positive specimen geometries, shows that the load ratio depends on the material by means of  $c_f$  and is independent of the specimen geometry if the characteristic dimension of the structure is expressed as  $D^{**}$ . Furthermore, when  $D^{**}$  is normalized to  $l_{ch}$ , the load ratio depends only on the parameter  $\kappa_f$  which is related to the shape of the softening curve.

Following Planas and Elices (1992), a lower limit of  $c_f$  is related to the critical crack opening  $w_c$

$$c_f \geq \frac{\pi}{32} w_c^2 \frac{E'}{G_F} \quad (10)$$

and expressing the critical crack opening in terms of characteristic crack opening as  $w_c = c_2 w_{ch} = c_2 G_F / f'_t$ , where  $c_2$  is a dimensionless parameter, Eq. 10 yields

$$c_f \geq \frac{\pi}{32} c_2^2 \frac{E' G_F}{f_t'^2} \quad (11)$$

and thus

$$\kappa_f \geq \frac{\pi}{32} c_2^2 \quad (12)$$

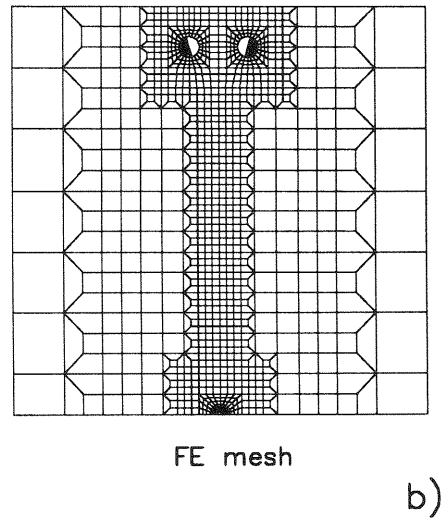
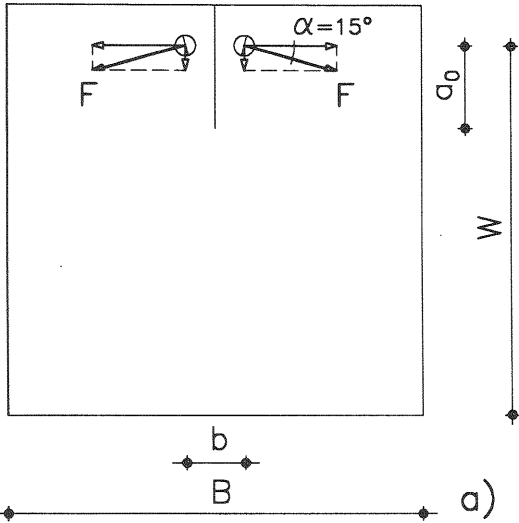
Using the lower bound value of  $\kappa_f$  from Eq. 12, Eq. 9 can be rewritten as

$$\frac{P_{\max}^{\text{LEFM}}}{P_{\max}^{\text{NLFM}}} \geq \left( 1 + \frac{\pi}{32} \frac{c_2^2}{\frac{D^{**}}{l_{ch}}} \right)^{\frac{1}{2}} \quad (13)$$

### 3 Comparison between theory and numerical results

The theoretical relations previously obtained are now contrasted with the results of a numerical parametric study on CT (Fig. 1a,b) and TPB specimens (Fig. 2) performed by Plizzari and Saouma (1995b) using MERLIN (Reich et al., 1994). The study referred to large specimens with different dimensions characterized by a bilinear softening law where the values of the governing parameters were changed, as summarized in Figs. 1c,d,e,f.

Fig. 3a shows the relationship between  $\kappa_f$  and  $D^{**}/l_{ch}$  as obtained by all the FE analyses with  $c_2 = 5$  that allowed a good fitting of several experimental results on concrete specimens (Plizzari and Saouma 1995). We observe that the numerical results diverge for increasing values of the  $D^{**}/l_{ch}$  ratio; this dispersion is in great part caused by the fact that, in all cases, the mesh topology was



Specim.	W [m]	a <sub>0</sub> [m]	B [m]	b [m]
25 ft.	6.86	1.52	7.62	1.08
50 ft.	13.72	3.04	15.24	2.16
100 ft.	27.44	6.08	30.48	4.32
200 ft.	54.88	12.16	60.96	8.64

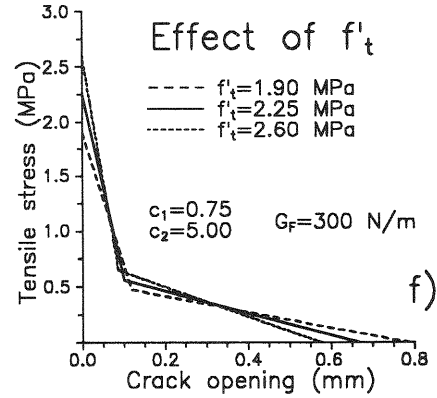
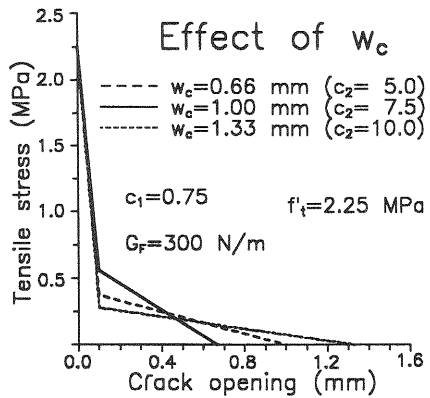
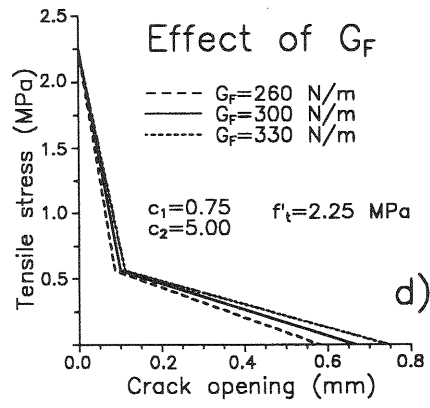


Fig.1. Mesh and dimensions adopted for the numerical parametric study of CT models (a,b,c), bilinear concrete softening law for the three considered values of fracture energy  $G_F$  (d), critical crack opening  $w_c$  (e) and tensile strength  $f'_t$  (f)

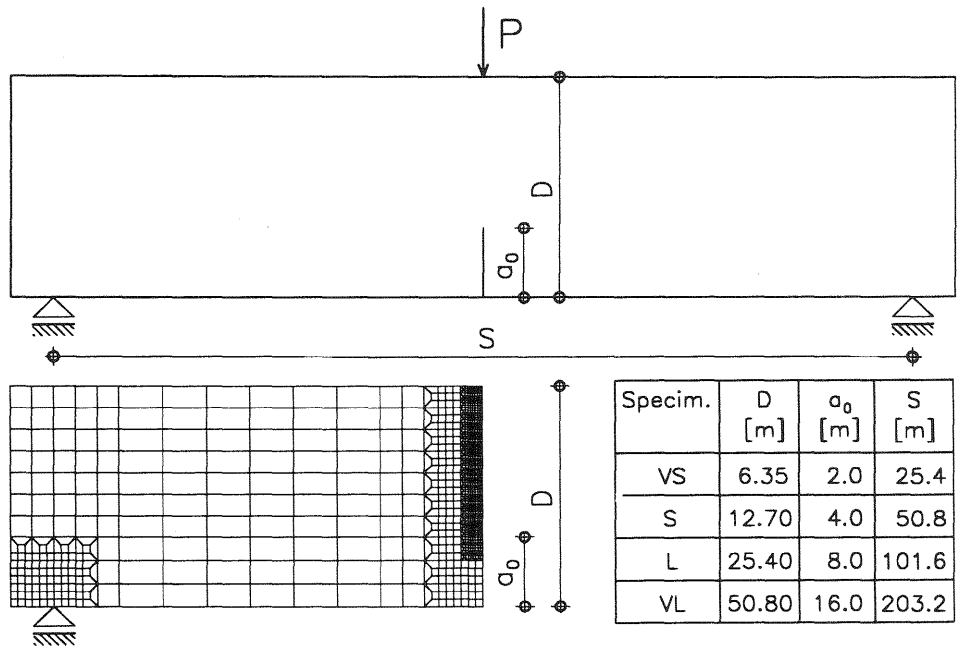


Fig.2. Meshes adopted for the numerical parametric study of Three Point Bending models

kept identical whereas the size was linearly scaled to accommodate larger  $D$  (Fig. 1b). As a result, larger models may not have a fine enough mesh at their crack tip to capture the FPZ and the effect of  $\kappa_f$  adequately. However, it should be noted that, for large models,  $\kappa_f$  varies between 1.5 and 2.0 (the value  $\kappa_f = 1.8$  was chosen as reference value). For  $c_2$  equal to 7.5 and 10,  $\kappa_f$  is larger but its value was not determined in that study since only few numerical results were available. From Eq. 12, a lower limit of  $\kappa_f$  corresponding to  $c_2 = 5$  is 2.45, which is higher than the numerically determined one, while for  $c_2 = 7.5$  and 10, the values of  $\kappa_f$  are 5.52 and 9.82 respectively.

Fig. 3b contrasts the theoretical prediction of the normalized geometry independent stress  $\bar{\sigma}_{N,D}/f'_t$ , as obtained by Eqs. 7, 8 for NLFM and LFM respectively, with all the numerical results obtained for both CT and TPB specimens. The theoretical results from Eq. 7 are plotted for different values of  $\kappa_f$ : 1.8, 2.45, 5.52 and 9.82. We observe that the theoretical LFM curve matches the numerical LFM results very well, and that the theoretical NLFM curve for  $\kappa_f = 1.8$  matches all the numerical NLFM results with

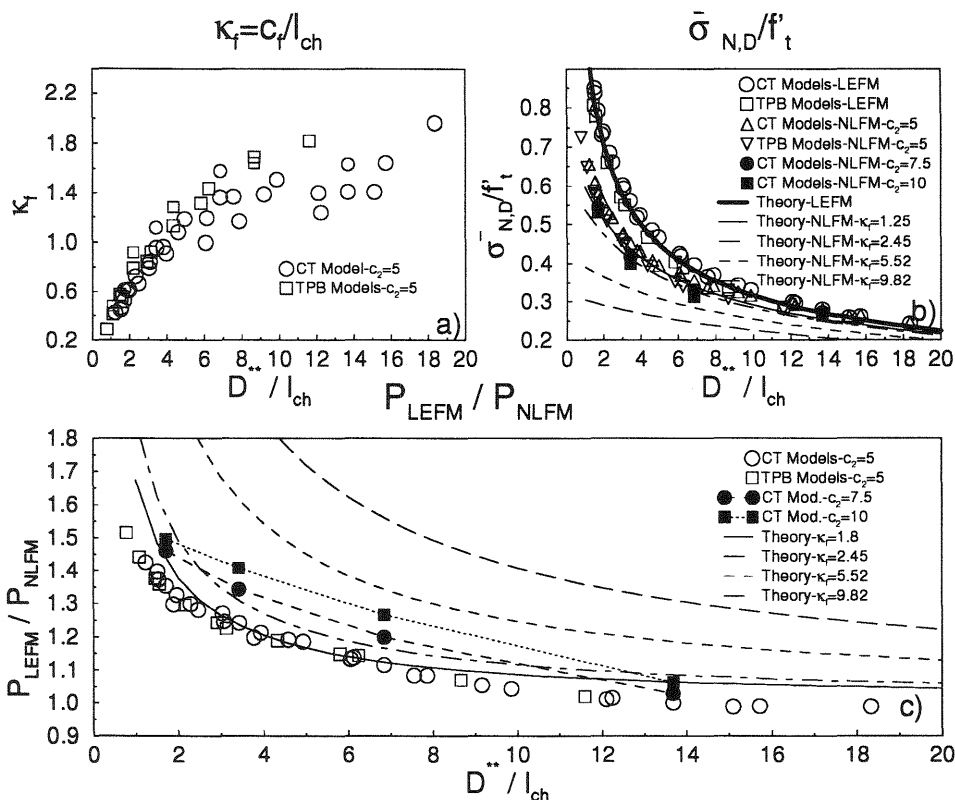


Fig.3. Comparison of the theoretical predictions with the numerical results

$c_2 = 5$ . Also, the theoretical curve for  $\kappa_f = 2.45$ , as obtained from Eq. 12, is very close to the numerical results. On the other hand, the curves for  $\kappa_f = 5.52$  and  $9.82$  underestimate the numerically determined maximum load; however, it should be noted that the adopted meshes probably become too coarse when a large  $w_c$  (and thus a large FPZ) is adopted since the FPZ develops in a very small number of elements.

Fig. 3c contrasts the theoretical predictions of the  $P_{\max}^{LEFM} / P_{\max}^{NLFM}$  (Eq. 9), with all the numerical results. Again, it should be noted that the theoretical curve matches well to all the numerical results obtained with  $c_2 = 5$  for both  $\kappa_f = 1.8$  and  $2.45$  when the  $D^*/l_{ch}$  ratio is larger than 3, and overestimates the error for smaller ratios. The same good match is not obtained with  $c_2 = 7.5$  and  $10$  but, as mentioned, the coarseness of the adopted mesh could have influenced the numerical results.

## 4 Concluding remarks

On the basis of the LEFM and NLFM scale laws for concrete, a theoretical expression to assess the error encountered in performing a LEFM analysis of a large concrete structure was proposed (Eq. 9). This very simple equation, valid for positive specimen geometries, shows that the load ratio  $P_{\max}^{\text{LEFM}} / P_{\max}^{\text{NLFM}}$ , which varies with structure dimension, depends only on the material and is independent of specimen geometry if the characteristic dimension of the structure is expressed in terms of  $D^{**}$ . Also, if  $D^{**}$  is normalized to the characteristic length of the material  $l_{ch}$ , the load ratio depends only on the parameter  $\kappa_f$  which is related to the shape of the softening curve.

A comparison with numerical results obtained by the authors (Plizzari and Saouma, 1985b; Fig. 3c), shows that the theoretical  $P_{\max}^{\text{LEFM}} / P_{\max}^{\text{NLFM}}$  ratio matches all the numerical results well when the  $D^{**}/l_{ch}$  ratio is larger than 3, and overestimates the error for smaller ratios.

## Acknowledgments

This research has been funded by the Electric Power Research Institute, Palo-Alto, through Research Contract No. RP-2917-08. The support of its program manager, Mr. Doug Morris, and its project monitor, Mr. Howard Boggs is gratefully acknowledged.

The first author would like to acknowledge the Commission for the Cultural Exchanges between Italy and the United States (Rome) and the Council for International Exchange of Scholars for their support for his stay at the University of Colorado at Boulder.

## Bibliography

- Bažant, Z.P. (1984) Size effect in blunt fracture: concrete, rock, metal. **ASCE Journal of Engineering Mechanics**, 110 (4), 518-535.
- Bažant, Z.P. and Kazemi, M.T. (1990) Determination of fracture energy, process zone length and brittleness number from size effect, with application to rock and concrete. **International Journal of Fracture**, 44, 111-131.

- Bažant, Z. P., Kim, J.K. and Pfeiffer, P.A. (1986), Determination of fracture properties from size effect tests. **ASCE Journal of Engineering Mechanics**, 112(2), 289-307.
- Carpinteri, A. (1982) Notch sensitivity in fracture testing of aggregative materials. **Engineering Fracture Mechanics**, 16, 467-481.
- Hillerborg, A. (1985) A comparison between the size effect law and the fictitious crack model, in **Dei Poli Anniversary Volume** (ed. L. Cedolin), Politecnico di Milano, 329-334.
- Hillerborg, A., Modéer, M. and Petersson, P.E. (1976) Analysis of crack formation and crack growth in concrete by means of fracture mechanics and finite elements. **Cement and Concrete Research**, 6, 773-782.
- Jenq, Y. S. and Shah, S. P. (1985) A two parameter fracture model for concrete. **ASCE Journal of Engineering Mechanics**, 111(10), 1227-1241.
- Planas, J. and Elices, M. (1988) Size-effect in concrete structures: mathematical approximations and experimental validation, in **Strain localization and size effect due to cracking and damage** (eds Z.P. Bažant and J. Masars), Elsevier Applied Science, London, 462-476.
- Planas, J. and Elices (1991) Nonlinear fracture of cohesive materials. **International Journal of Fracture**, 44, 111-131.
- Planas, J. and Elices (1992) Asymptotic analysis of a cohesive crack: 1. Theoretical background. **International Journal of Fracture**, 51, 139-157.
- Plizzari, G.A. and Saouma V.E. (1995) Application of fracture mechanics to concrete structures- Part I: Normal size structures. Submitted for publication to **ASCE Journal of Structural Engineering**.
- Plizzari, G.A. and Saouma V.E. (1995b) Application of fracture mechanics to concrete structures- Part II: Large structures. Submitted for publication to **ASCE Journal of Structural Engineering**.
- Reich, R., Červenka, J. and Saouma, V.E. (1994) MERLIN, A three-dimensional finite element program based on a mixed-iterative solution strategy for problems in elasticity, plasticity and linear and nonlinear fracture mechanics. **Technical report** submitted to EPRI, Palo Alto, CA, USA, University of Colorado at Boulder.
- Smith, E. (1995) The size effect expression for an elastic-softening material. **Mechanics of Materials**, 19, 261-270.